Taylor & Francis
Taylor & Francis Group

RESEARCH PAPER

Check for updates

Effect of glycation focusing on the process of epidermal lipid synthesis in a reconstructed skin model and membrane fluidity of stratum corneum lipids

Mami Yokota[a], Hitoshi Masaki[b], Yuri Okano[b], and Yoshihiro Tokudome[a]

[a]Laboratory of Dermatological Physiology, Faculty of Pharmaceutical Sciences, Josai University, Sakado, Saitama, Japan; [b]School of Bioscience and Biotechnology, Tokyo University of Technology, Hachioji, Tokyo, Japan

ABSTRACT

We previously reported that epidermal glycation causes an increase in saturated fatty acid (FA) content in a differentiated reconstructed skin model and HaCaT cells. However, the relationship between ceramides (CERs) and glycation and their effects on stratum corneum (SC) barrier function was not elucidated. In this study, we investigated the effect of glycation on lipid content in 6-day-old cultured reconstructed skin. We used the EPISKIN RHE 6D model and induced glycation using glyoxal. In addition to transepidermal water loss, content of CERs, cholesterol and FA in the reconstructed epidermal model were analyzed by high performance thin layer chromatography. Expression of genes related to ceramide metabolism was determined by real time RT-PCR. Membrane fluidity of stratum corneum lipid liposomes (SCLL) that mimic glycated epidermis was analyzed using an electron spin resonance technique. It was found that FA was significantly increased by glycation. CER[NS], [AP], and cholesterol were decreased in glycated epidermis. Expression of ceramide synthase 3 (CERS3) was significantly decreased while fatty acid elongase 3 was increased by glyoxal in a dose dependent manner. Membrane fluidity of SCLL mimicking the lipid composition of glycated epidermis was increased compared with controls. Therefore, disruption of CER and FA content in glycated epidermis may be regulated via CERS3 expression and contribute to abnormal membrane fluidity.

Introduction

Viable epidermis has a unique mechanism of lipid metabolism and contributes to the production of the stratum corneum (SC). As the outermost layer of the skin, the SC is essential for protecting the host from external stimuli including ultraviolet light, chemicals, mechanical insults, and pathogens, as well as preventing loss of water from the body.[1] In the SC, corneocytes are embedded in an intercellular lipid matrix, composed of approximately equimolar concentrations of various species of ceramides (CERs), cholesterol (chol) and fatty acids (FAs), forming a lamellar structure.[2,3] These lipids, derived from both epidermal biosynthesis and intake from other organs, are delivered to the extracellular space by the exocytosis of lamellar bodies, containing phospholipids, glucosylceramides, sphingomyelin, chol, and enzymes. At the extracellular space, these lipids are metabolized by enzymes to lamellar forming lipids.[4-8]

Importantly, the change in the ratio and constitution of these SC intercellular lipids contributes to the exacerbation of skin diseases. For example, all 3 key lipids are decreased in patients with atopic dermatitis (AD).[9-12] Not only these key lipids, but also the composition of sphingoid bases, sphingosine and sphinganine which are precursors and catabolites of CER, influences lamellar membrane architecture in AD derived SC, contributing to the barrier abnormality.[13] Furthermore, natural aging and photoaging also cause disruption of lipid content.[14,15] Thus, maintaining the homeostasis of lipid metabolism is essential for proper barrier function in skin.

Advanced glycation end products (AGEs) are generated via the non-enzymatic Maillard reaction between the aldehyde group of reducing sugars and amino group of proteins, lipids or nucleic acids.[16] As the population ages, accumulation of AGEs in tissues has attracted much attention as a cause of diabetic complications and are also thought to be related to other lifestyle-related diseases. For skin, where AGEs can be seen, developing an anti-AGEs strategy is important from an aesthetic as well as a functional point of view. AGEs accumulate in both dermis (e.g. collagen and elastic fibers) and epidermis (e.g. keratin 10).[17-19] Additionally, AGEs can be ligands for receptor for AGEs (RAGE) and provoke inflammatory signaling via a reactive oxygen species (ROS) / nuclear factor-κB (NF-κB) pathway.[20-22] Recently, hyperglycemia has been reported to be strongly related to disruption of lipid metabolism. Findings show that hyperglycemia contributes to lipotoxicity via upregulation of FA production, causing endoplasmic reticulum (ER) stress and apoptosis of pancreatic β cells.[23,24] Thus, it is expected that the lipid metabolism in glycated epidermis is also disrupted, but there are few studies regarding glycation in skin.[25] We previously reported that FA content in glyoxal (GO) treated HaCaT cells and a reconstructed skin model was significantly increased.[26] However, the relationship between metabolism of FAs and other lipids and the mechanisms of barrier disruption in glycated epidermis remain to be elucidated.

Here, we revealed the relationship between the extent of glycation and metabolism of various SC intercellular lipids and its effect on barrier function using a reconstructed skin model and SC lipid liposomes (SCLLs) mimicking the intercellular lamellae structure.

Materials and methods

Reagents

GO, chol and palmitic acid were purchased from Wako Pure Chemical Industries, Ltd. (Osaka, Japan). For lipid standards, Ceramide[NS] and [AS] were purchased from Matreya (State College, PA, USA) and Ceramide[NP] and [AP] were purchased from Evonic Industries AG (Essen, Germany). Chol, cholesterol sulfate, palmitic acids for liposome and 5-DOXYL-

stearic acid were purchased from Sigma-Aldrich (St. Louis, MO, USA).

Cell culture

The reconstructed epidermal model 6D RHE and EPISKIN were purchased from EPISKIN (Lyon, France) and maintained in the supplied culture medium in a humidified atmosphere of 5% CO_2 at 37°C. AGEs were induced by exposure to various concentrations of GO in culture medium for 72 h from the basal side.

Cell viability assay

Reconstructed model epidermis was cultured for 24 h before exposure to various concentrations of GO from the basal side. After 72 h incubation, cells were washed with culture medium and incubated with alamar Blue® in culture medium (1:10) for a further 4 h. The fluorescence at Ex. 570 nm, Em. 585 nm, of the medium was measured using a microplate reader (SpectraMax M2^e, Molecular Devices, Sunnyvale, CA, USA).

RNA extraction and quantitative real time PCR

Total RNA was isolated from the reconstructed epidermal model using RNAiso Plus (Takara Bio, Otsu, Shiga, Japan), followed by reverse transcription to cDNA using the PrimeScript® RT reagent kit (Takara Bio) on a thermal cycler (Veriti, Applied Biosystems, Foster City, CA, USA). Real-time PCR reactions were performed using SYBR® Premix Ex Taq^{TM} (Takara Bio) on a StepOnePlus^{TM} (Applied Biosystems) with the respective primers (Table S1). The fold-change of expression was calculated according to the $\Delta\Delta C_T$ method using glyceraldehyde-3-phosphate dehydrogenase (GAPDH) as an endogenous control.

Lipid extraction

Epidermal lipid samples from reconstructed epidermal models were extracted in $CHCl_3$/MeOH 2:1 (v/v) solution after being washed and excised from the transwell. Samples were minced then sonicated for 10 min, the solution filtrated with a 0.22 μm pore filter membrane and dried under N_2 stream. All lipid extracts and standards were dissolved in $CHCl_3$/MeOH 2:1 (v/v) solution.

High Performance Thin Layer Chromatography (HPTLC) analysis

Ten μL of lipid extracts were applied to the HPTLC plate (HPTLC Silica gel 60, Merck Millipore, Darmstadt, Germany) together with lipids standards to generate calibration curves and developed twice in a saturated chromatographic chamber containing $CHCl_3$/MeOH/CH_3COOH 190:9:1 (v/v) mobile phase. Then the HPTLC plate was dried and sprayed with a reagent (10% $CuSO_3$, 8% H_3PO_4 aqueous solution) and heated to 180°C for 10 min and quantitated by densitometry using ChemiDoc[TM] XRS+ and Image Lab[TM] software (Bio-Rad, Hercules, CA, USA).

Measurement of transepidermal water loss (TEWL)

Cutaneous water evaporation was measured with a VAPOSCAN AS-VT100RS (Asahibiomed, Tokyo, Japan). Reconstructed epidermal models were naturalized for 1 h before measurements. ΔTEWL means TEWL at 72 h after GO exposure subtracted from TEWL before exposure to GO.

Liposome preparation

SCLL were prepared according to the conventional thin-film hydration method. Individual lipids were dissolved in chloroform/methanol (2:1) as shown in Table 1. The solvent was dried under reduced pressure using a rotary evaporator, leaving a thin film in the flask. The lipid film was hydrated with PBS, followed by freeze/thawing 5 times. The obtained large unilamellar vesicles were subjected to extrusion through polycarbonate filters using an extruder (pore size: 100, 200, and 400 nm, Merck Millipore). Particle diameter, PdI and ζ potential were measured using a Zetasizer Nano ZS (Malvern, Worcestershire, UK).

Electron spin resonance analysis

SCLLs were probed with 5-doxylstearic acid (5-DSA). 5-DSA was dissolved in methanol and thin films produced by evaporation under low pressure before mixing with SCLL for 5 min at RT. Probed SCLLs were then added to a capillary tube (HIRSCHMANN, Eberstadt, Germany) and sealed with putty (Terumo, Tokyo, Japan). After the samples were inserted, electron spin resonance (ESR) spectra were recorded on a RFR-30 (Radical Research Inc., Tokyo, Japan). The operating conditions of the equipment were: microwave power of 4.0 mW, modulation frequency of 9.43 kHz, modulation amplitude of 0.2 mT, magnetic field scan of 337.5 mT, sweep time of 8 min, detector time constant of 0.1 ms, at RT. To determine the liposomal fluidity, the S value was determined using the following equation Eq. 1, Fig. S1).

$$S = 1/2(3\cos^2\theta - 1)$$
$$= (A_{//} - A_{\perp})/\{A_{zz} - (A_{xx} + A_{yy})/2\} \times 10$$
$$= (2T_{//}/2 - 2T_{\perp}/2)/\{33.6 - (6.3 + 5.8)/2\} \times 10$$
$$(1)$$

Data analysis

Statistical differences between groups were assessed by means of Dunnett's test (vs 0 mM treated group) or 2-tailed Student t-test using SAS University edition (SAS Institute, Cary, NC, USA). P value of < 0.05 was considered as the limit of statistical significance.

Results

Evaluation of barrier function in a glycated reconstructed epidermal model

To elucidate the barrier function of glycated epidermis, the RHE 6D model was exposed to various concentrations of GO from the basal side for 72 h. Cell viability was decreased in a GO concentration dependent manner (Fig. 1a, $p < 0.001$) compared with the untreated control. The ΔTEWL of the glycated model indicated a significant decrease in TEWL in the 0.5 mM and 1 mM GO exposed groups (Fig. 1b, $p < 0.05$, $p < 0.001$ respectively).

Quantification of lipids in the glycated 6D RHE model

Lipids were extracted from the 6D RHE model and separated by HPTLC to quantitate the content of CERs, FA and Chol (Fig. 2). In the 6D RHE model, the

Table 1. Formulation and fluidity of liposomes mimicking normal (SCLL) and glycated (G-SCLL) epidermal lipid composition. Results are expressed as the mean $\pm$ SD of n = 3 replicates.[*] $p < 0.05$.

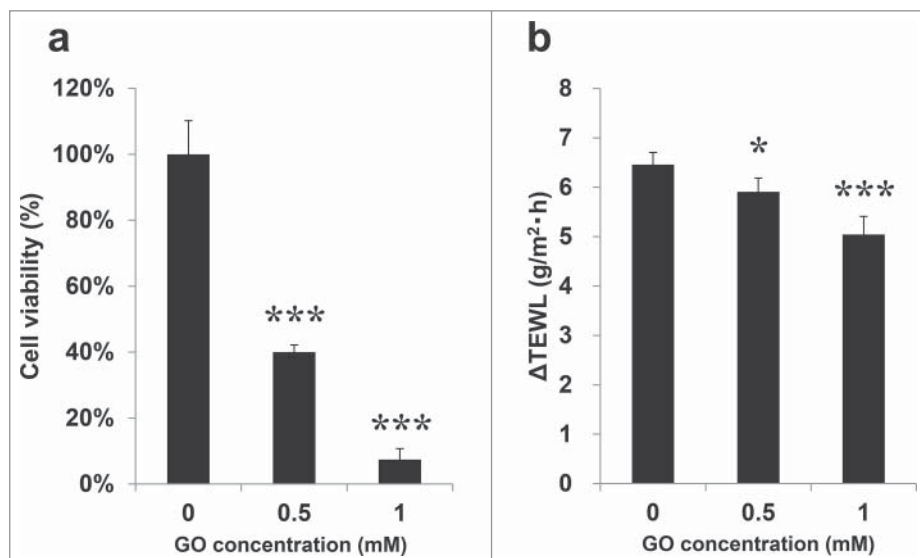|	Composition	Ratios by weight	S
SCLL	CER[NS]/Chol/PA/CholSE	40/40/25/10	1.364 ± 0.005
G-SCLL	CER[NS]/Chol/PA/CholSE	20/20/50/5	$1.316 \pm 0.004^*$

Figure 1. General properties of the glycated reconstructed epidermal model. Glycation was induced by hydration with various concentrations of GO from the basal side for 72 h. Viability of glycated 6D RHE was measured by alamar Blue® assay(a). ΔTEWL of glycated 6D RHE was measured using vaposcan (b). All results are expressed as the mean ± SD of n = 3 or n = 4 replicates, respectively. $^*p < 0.05$, $^{***}p < 0.001$.

content of CER[NS], [AP]b was decreased in glycated skin. Contents of these lipids in the normal epidermal model were 27.41 and 14.69 $\mu g/cm^2$ respectively, while in the glycated epidermal model they were 18.45 ($p <$

0.05) and 10.18 ($p < 0.05$) $\mu g/cm^2$, respectively (Fig. 2a and e). Chol content also decreased in the glycated epidermal model; the normal epidermal model contained 40.97 $\mu g/cm^2$ and the glycated contained

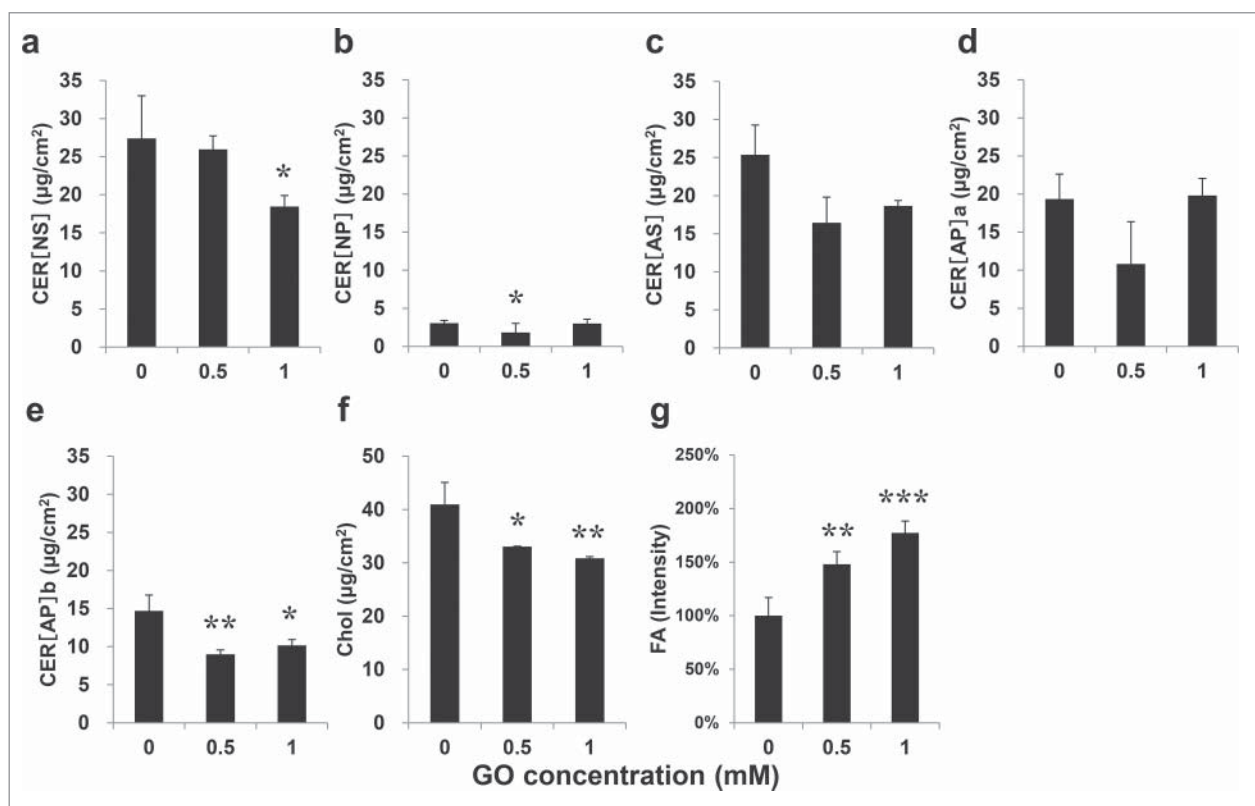**Figure 2.** Changes in the content of epidermal lipids in glycated reconstructed epidermal model. Lipids contents of 6D RHE were determined after 72 h exposure to glyoxal by HPTLC: CER[NS] (a), CER[NP] (b), CER[AS] (c), CER[AP]a (d), CER[AP]b (e), cholesterol (f), and fatty acids (g). All results are expressed as the mean ± SD of n = 3 replicates. $^*p < 0.05$, $^{**}p < 0.01$, $^{***}p < 0.001$.

30.85 μg/cm^2 ($p < 0.01$, Fig. 2f). Furthermore, the relative FA content was 1.8 times higher in glycated (1 mM GO exposed) epidermal model compared with the untreated control ($p < 0.001$, Fig. 2g).

Changes in expression of genes related to lipid metabolism

To elucidate the mechanisms of change in lipid contents in glycated skin, the mRNA expression in EPISKIN was measured by real time PCR. Expression of CER synthase 3 (*CERS3*) was 0.44-fold decreased in 1 mM GO exposed epidermis, while acid ceramidase (*aCDase*) was not significantly changed (Fig. 3a, 3b). FA elongase, *ELOVL3*, was increased 2.78-fold in glycated epidermis, while no significant difference was shown in *ELOVL4* (Fig. 3c and d). Expression of fatty acid synthase (*FASN*), which is important for synthesis of C16 FA, was 0.13-fold decreased by GO exposure ($p < 0.001$, Fig. 3e).

Characterization of features of normal and glycated epidermis mimicking SCLL

Finally, the relationship between lipid composition and lamellar stability was investigated using SCLL by ESR methods. Measurement of SCLL particle diameter, PdI and ζ potential showed that both normal SCLL and SCLL mimicking glycated epidermis (G-SCLL) were stable at 37°C for at least 1 w (Fig. S1a-c). However, order parameter S of G-SCLL, determined by ESR spectrum of 5-DSA, was significantly decreased compared with SCLL, indicating higher membrane fluidity ($p < 0.05$) (Table 1, Fig. S1).

Discussion

In the present study, we investigated the effect of glycation on epidermal CERs metabolism and found differences in lipid metabolism and barrier function. Glycation of keratinocytes causes a decrease in cell
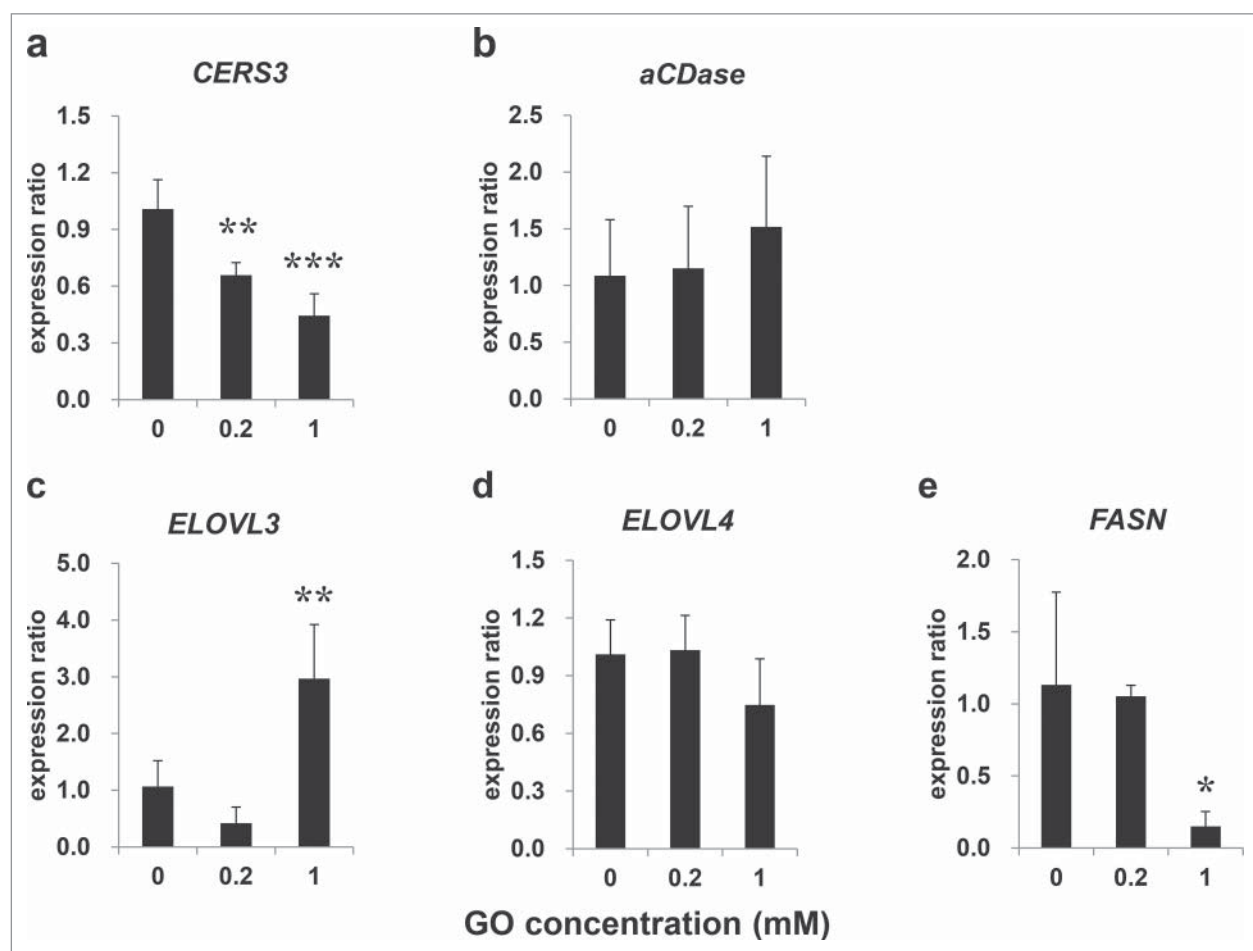

Figure 3. Expression of ceramide and fatty acid metabolism-associated genes. Expression of *CERS3* (a), *aCDase* (b), *ELOVL3* (c) *ELOVL4* (d) and *FASN* (e) in EPISKIN after 72 h exposure to glyoxal as determined by real-time RT PCR. All results are expressed as the mean $\pm$ SD of n = 3 replicates. $^*p < 0.05$, $^{**}p < 0.01$, $^{***}p < 0.001$.

viability via apoptotic pathway [22]. Cell viability and ΔTEWL of GO treated reconstructed skin were significantly decreased in a dose dependent manner. Interestingly, we did not find any color change in this experiment at the concentrations of GO used, but found that exposure to 5 mM GO is required for a yellowish color change, which is characteristic of glycated skin, of the reconstructed epidermal model in a pilot study (data not shown). From these results, changes in lipid metabolism may occur before alteration in appearance, thus early treatment of skin glycation is thought to be important.

The content of FA in early glycated skin was significantly increased as previously reported[26] and glycated 6D RHE also showed an increase in FA content. In addition to upregulation of *ELOVL3*, the downregulation of *CERS3* may contribute to the accumulation of FA and lowering of CER content. Although ceramides in skin are produced via either the *de novo* or salvage pathways,[27,28] CERSs control both the *de novo* synthesis of sphingolipids as well as the recycling of sphingosine from the breakdown of preformed sphingolipids. Of the 6 types of CERSs reported, CERS3 and CERS4 are distributed in epidermis[29] and deficiency of CERS3 in mice revealed the lack of 90% of epidermal CERs.[30] Since expression of *aCDase* was not changed in our experiment (Fig. 3), it is suggested that the synthetic pathway plays an important role in the decrease in CERs contents. ELOVL3 and CERS3 have substrate specificity to saturated FA: C18:0, C20:0, C22:0, C24:0 for ELOVL3[31] and C16:0, C18:0, C22:0, C24:0 and >C26 for CERS3.[29] This preference may explain the increase of C16:0, C18:0 FA. EPISKIN, which was used to measure the mRNA expression in the reconstructed skin model, showed no significant difference in CERs content (data not shown). Notably, this model already has mature SC, including various ceramides, and the cultured cells cannot undergo turnover. Thus, existing ceramides might mask the change in ceramides contents, although expression of *CERS3* was significantly decreased. Park *et al.* reported that FA and cholesterol contents were decreased and ceramide contents was not changed by glycation using a spontaneously diabetic rat strain with typical characteristics of type 2 diabetes mellitus.[25] To understand the differences in our results, species differences and method for AGEs induction should be taken into account in future studies.

Our SCLL model had a lipid composition that mimicked glycated epidermis, demonstrating slight but higher membrane fluidity compared with untreated controls (Table 1, Fig. S1). Thus, the contribution of change in lamellar lipid fluidity to an increase in TEWL is expected. We previously reported that the barrier to low molecular weight hydrophilic compounds in *in vitro* glycated full-thickness skin was disrupted and conformational change in intercellular lipids contributed to this phenomenon.[26,32] Taken together, this study successfully connected the disruption of lipid synthesis in viable epidermis to SC lamellar fluidity. Our results suggest the glycation-induced disruption of SC structure and lipid homeostasis. However, it is well documented that percutaneous penetration occurs through transcellular, and to a lesser extent, appendageal routes as well as intracellular routes.[33] Since AGEs in epidermis accumulate at keratin 10,[17] non-physiologic crosslinking of keratin may also be involved in barrier function. Additionally, the effect of AGEs on appendage should be elucidated in the near future.

Abbreviations

AD	Atopic dermatitis
AGE	Advanced glycation end products
CER	Ceramide
Chol	Cholesterol
5-DSA	5-DOXYL stearic acid
ESR	Electron skin resonance
FA	Fatty acids
GO	Glyoxal
SCLL	Stratum corneum lipid liposome
TEWL	Transepidermal water loss

Disclosure of potential conflicts of interest

No potential conflicts of interest were disclosed.

Acknowledgments

References

[1] Feingold KR. Thematic review series: Skin lipids. The role of epidermal lipids in cutaneous permeability barrier homeostasis. J Lipid Res 2007; 48:2531-46; PMID:17872588; https://doi.org/10.1194/jlr.R700013-JLR200

[2] Swartzendruber DC, Wertz PW, Kitko DJ, Madison KC, Downing DT. Molecular models of the intercellular lipid lamellae in mammalian stratum corneum. J Invest Dermatol 1989; 92:251-7; PMID:2918233; https://doi.org/10.1111/1523-1747.ep12276794

[3] Bouwstra JA, Gooris GS, Bras W, Downing DT. Lipid organization in pig stratum corneum. J Lipid Res 1995; 36:685-95; PMID:7542308

[4] Elias PM, Feingold KR, Fartasch M. Epidermal lamellar body as a multifunctional secretory organelle. In: Elias PM, Feingold KR, ed. Skin barrier. New York: Taylor & Francis, 2006:261-72.

[5] Freinkel RK, Traczyk TN. Lipid composition and acid hydrolase content of lamellar granules of fetal rat epidermis. J Invest Dermatol 1985; 85:295-8; PMID:4045218; https://doi.org/10.1111/1523-1747.ep12276831

[6] Grayson S, Johnson-Winegar AG, Wintroub BU, Isseroff RR, Epstein EH Jr, Elias PM. Lamellar body-enriched fractions from neonatal mice: preparative techniques and partial characterization. J Invest Dermatol 1985; 85:289-94; PMID:4045217; https://doi.org/10.1111/1523-1747.ep12276826

[7] Wertz PW. Epidermal lipids. Semin Dermatol 1992; 11:106-13; PMID:1498013

[8] Wertz PW, Downing DT, Freinkel RK, Traczyk TN. Sphingolipids of the stratum corneum and lamellar granules of fetal rat epidermis. J Invest Dermatol 1984; 83:193-5; PMID:6470524; https://doi.org/10.1111/1523-1747.ep12263553

[9] Imokawa G. A possible mechanism underlying the ceramide deficiency in atopic dermatitis: Expression of a deacylase enzyme that cleaves the N-acyl linkage of sphingomyelin and glucosylceramide. J Dermatol Sci 2009; 55:1-9; PMID:19443184; https://doi.org/10.1016/j.jdermsci.2009.04.006

[10] Imokawa G, Abe A, Jin K, Higaki Y, Kawashima M, Hidano A. Decreased level of ceramides in stratum corneum of atopic dermatitis: An etiologic factor in atopic dry skin? J Invest Dermatol 1991; 96:523-6; PMID:2007790; https://doi.org/10.1111/1523-1747.ep12470233

[11] Di Nardo A, Wertz P, Giannetti A, Seidenari S. Ceramide and cholesterol composition of the skin of patients with atopic dermatitis. Acta Derm Venereol 1998; 78:27-30; PMID:9498022; https://doi.org/10.1080/00015559850135788

[12] Elias PM. Lipid abnormalities and lipid-based repair strategies in atopic dermatitis. Biochim Biophys Acta 2014; 1841:323-30; PMID:24128970; https://doi.org/10.1016/j.bbalip.2013.10.001

[13] Loiseau N, Obata Y, Moradian S, Sano H, Yoshino S, Aburai K, Takayama K, Sakamoto K, Holleran WM, Elias PM, et al. Altered sphingoid base profiles predict compromised membrane structure and permeability in atopic dermatitis. J Dermatol Sci 2013; 72:296-303; PMID:24070864; https://doi.org/10.1016/j.jdermsci.2013.08.003

[14] Kim EJ, Jin XJ, Kim YK, Oh IK, Kim JE, Park CH, Chung JH. UV decreases the synthesis of free fatty acids and triglycerides in the epidermis of human skin in vivo, contributing to development of skin photoaging. J Dermatol Sci 2010; 57:19-26; PMID:19932008; https://doi.org/10.1016/j.jdermsci.2009.10.008

[15] Kim EJ, Kim MK, Jin XJ, Oh JH, Kim JE, Chung JH. Skin aging and photoaging alter fatty acids composition, including 11,14,17-eicosatrienoic acid, in the epidermis of human skin. J Korean Med Sci 2010; 25:980-3; PMID:20514327; https://doi.org/10.3346/jkms.2010.25.6.980

[16] Gkogkolou P, Bohm M. Advanced glycation end products: Key players in skin aging? Dermatoendocrinol 2012; 4:259-70; PMID:23467327; https://doi.org/10.4161/derm.22028

[17] Kawabata K, Yoshikawa H, Saruwatari K, Akazawa Y, Inoue T, Kuze T, Sayo T, Uchida N, Sugiyama Y. The presence of N(epsilon)-(Carboxymethyl) lysine in the human epidermis. Biochim Biophys Acta 2011; 1814:1246-52; PMID:21708295; https://doi.org/10.1016/j.bbapap.2011.06.006

[18] Verzijl N, DeGroot J, Thorpe SR, Bank RA, Shaw JN, Lyons TJ, Bijlsma JW, Lafeber FP, Baynes JW, TeKoppele JM. Effect of collagen turnover on the accumulation of advanced glycation end products. J Biol Chem 2000; 275:39027-31; PMID:10976109; https://doi.org/10.1074/jbc.M006700200

[19] Yoshinaga E, Kawada A, Ono K, Fujimoto E, Wachi H, Harumiya S, Nagai R, Tajima S. N(varepsilon)-(carboxymethyl)lysine modification of elastin alters its biological properties: Implications for the accumulation of abnormal elastic fibers in actinic elastosis. J Invest Dermatol 2012; 132:315-23; PMID:21956123; https://doi.org/10.1038/jid.2011.298

[20] Lohwasser C, Neureiter D, Weigle B, Kirchner T, Schuppan D. The receptor for advanced glycation end products is highly expressed in the skin and upregulated by advanced glycation end products and tumor necrosis factor-alpha. J Invest Dermatol 2006; 126:291-9; PMID:16374460; https://doi.org/10.1038/sj.jid.5700070

[21] Leibold JS, Riehl A, Hettinger J, Durben M, Hess J, Angel P. Keratinocyte-specific deletion of the receptor RAGE modulates the kinetics of skin inflammation in vivo. J Invest Dermatol 2013; 133:2400-6; PMID:23594597; https://doi.org/10.1038/jid.2013.185

[22] Zhu P, Ren M, Yang C, Hu YX, Ran JM, Yan L. Involvement of RAGE, MAPK and NF-kappaB pathways in AGEs-induced MMP-9 activation in HaCaT keratinocytes. Exp Dermatol 2012; 21:123-9; PMID:22229442; https://doi.org/10.1111/j.1600-0625.2011.01408.x

[23] Wang H, Kouri G, Wollheim CB. ER stress and SREBP-1 activation are implicated in beta-cell glucolipotoxicity. J Cell Sci 2005; 118:3905-15; PMID:16091421; https://doi.org/10.1242/jcs.02513

[24] Cui W, Ma J, Wang X, Yang W, Zhang J, Ji Q. Free fatty acid induces endoplasmic reticulum stress and apoptosis of beta-cells by Ca2+/calpain-2 pathways. PloS One

2013; 8:e59921; PMID:23527285; https://doi.org/10.1371/journal.pone.0059921

[25] Park HY, Kim JH, Jung M, Chung CH, Hasham R, Park CS, Choi EH. A long-standing hyperglycaemic condition impairs skin barrier by accelerating skin ageing process. Exp Dermatol 2011; 20:969-74; PMID:22017743; https://doi.org/10.1111/j.1600-0625.2011.01364.x

[26] Yokota M, Tokudome Y. The effect of glycation on epidermal lipid content, its metabolism and change in barrier function. Skin Pharmacol Physiol 2016; 29:231-42; PMID:27548800; https://doi.org/10.1159/000448121

[27] Rabionet M, Gorgas K, Sandhoff R. Ceramide synthesis in the epidermis. Biochim Biophys Acta 2014; 1841:422-34; PMID:23988654; https://doi.org/10.1016/j.bbalip.2013.08.011

[28] Taniguchi M, Okazaki T. The role of sphingomyelin and sphingomyelin synthases in cell death, proliferation and migration-from cell and animal models to human disorders. Biochim Biophys Acta 2014; 1841:692-703; PMID:24355909; https://doi.org/10.1016/j.bbalip.2013.12.003

[29] Mullen TD, Hannun YA, Obeid LM. Ceramide synthases at the centre of sphingolipid metabolism and biology. Biochem J 2012; 441:789-802; PMID:22248339; https://doi.org/10.1042/BJ20111626

[30] Jennemann R, Rabionet M, Gorgas K, Epstein S, Dalpke A, Rothermel U, Bayerle A, van der Hoeven F, Imgrund S, Kirsch J, et al. Loss of ceramide synthase 3 causes lethal skin barrier disruption. Hum Mol Genet 2012; 21:586-608; PMID:22038835; https://doi.org/10.1093/hmg/ddr494

[31] Mizutani Y, Mitsutake S, Tsuji K, Kihara A, Igarashi Y. Ceramide biosynthesis in keratinocyte and its role in skin function. Biochimie 2009; 91:784-90; PMID:19364519; https://doi.org/10.1016/j.biochi.2009.04.001

[32] Yokota M, Tokudome Y. Permeation of hydrophilic molecules across glycated skin is differentially regulated by the stratum corneum and epidermis-dermis. Biol Pharm Bull 2015; 38:1383-8; PMID:26328494; https://doi.org/10.1248/bpb.b15-00372

[33] Barry BW. Mode of action of penetration enhancers in human skin. J Control Release 1987; 6:85-97; https://doi.org/10.1016/0168-3659(87)90066-6